Molecular and Cellular Neuroscience 77 (2016) 95–104

Contents lists available at ScienceDirect

Molecular and Cellular Neuroscience

journal homepage: www.elsevier.com/locate/ymcne

Evidence for a role of glycoprotein M6a in dendritic spine formation and synaptogenesis

Karina Formoso, Micaela D Garcia, Alberto C Frasch, Camila Scorticati *

Instituto de Investigaciones Biotecnológicas-Instituto Tecnológico de Chascomús (IIB –INTECH), Universidad Nacional de San Martín (UNSAM), Consejo Nacional de Investigaciones Científicas y Técnicas (CONICET), Buenos Aires, Argentina

ARTICLE INFO

Article history:
Received 14 July 2016
Revised 27 September 2016
Accepted 24 October 2016
Available online 26 October 2016

Keywords:
PLP family
Transmembrane domains
Synapses
nsSNPs variants
Dendritic arborization

ABSTRACT

Neuronal glycoprotein M6a belongs to the tetraspan proteolipid protein (PLP) family. Mutations in *GPM6A* gene have been related to mental disorders like schizophrenia, bipolar disorders and claustrophobia. M6a is expressed mainly in neuronal cells of the central nervous system and it has been extensively related to neuronal plasticity. M6a induces neuritogenesis and axon/filopodium outgrowth; however its mechanism of action is still unresolved. We recently reported that the integrity of the transmembrane domains (TMDs) 2 and 4 are critical for M6a filopodia induction. There is also experimental data suggesting that M6a might be involved in synaptogenesis. In this regard, we have previously determined that M6a is involved in filopodia motility, a process that is described in the first step of the filopodial model for synaptogenesis. In this work we analyzed the possible involvement of M6a in synaptogenesis and spinogenesis, and evaluated the effect of two non-synonymous SNPs present in the coding region of TMD2-*GPM6A* in these processes. The results showed that endogenous M6a colocalized with both, pre-synaptic (synaptophysin) and post-synaptic (NMDA-R1), markers along of neuronal soma and dendrites. M6a-overexpressing neurons displayed an increased number of synaptophysin and NMDA-R1 puncta and, also, an increased number of colocalization puncta between both markers. Conversely, the number of synaptic puncta markers in neurons expressing nsSNP variants was similar to those of control neurons. Overexpression of M6a is accompanied by an increase in spine density, particularly in mature spines, as compared with neurons expressing mGFP or *GPM6A* nsSNP variants. Taken together, these results suggest that M6a contributes positively to spine and, likely, synapse formation.

1. Introduction

Membrane glycoprotein M6a is a member of the proteolipid protein (PLP) family, which has been related to neuronal development in different experimental models. It is well-known that M6a induces neuritogenesis and axon and filopodia outgrowth in M6a-overexpressing neurons (Alfonso et al., 2005a; Lagenaur et al., 1992; Michibata et al., 2009; Sato et al., 2011a; Scorticati et al., 2011). The interest in studying M6a raises when variations in human *GPM6A* gene expression and non-coding single nucleotide polymorphisms (SNPs) were linked to mental disorders such as depression, schizophrenia and mental retardation (Boks et al., 2008; Fuchsova et al., 2015; Greenwood et al., 2012; Gregor et al., 2014).

Few studies have analyzed the relationship between M6a structure and its function. M6a is composed of 278 amino acids that form four transmembrane domains (TMDs), two external loops, and the N- and C-terminal regions located in the cell cytoplasm (Fig. 5B). Regarding its TMDs, Sato et al. demonstrate that M6a overexpression in COS-7 cells induces filopodial protrusions and that specific amino acids residues scattered throughout the N-terminal and the TMD1 are required (Sato et al., 2011b). We recently reported that certain glycines presents in TMD2 and TMD4 are needed for M6a self-interaction, oligomerization and filopodia induction in cultured hippocampal neurons. Three non-synonymous SNPs (nsSNPs) present in the coding region of TMD2 and TMD3 of *GPM6A* were found to affect M6a stability, interactions, localization and filopodia formation in neurons (Formoso et al., 2015).

Neuronal development involves neurite extension, axonal polarization and growth, dendritic arborization and synapse formation (Caceres et al., 2012; Gartner et al., 2014). Dendritic spines represent the post-synaptic compartment that commonly receives input from a single excitatory axon at the synapse. Spines are small protrusions, rich in actin filaments, which arise from the dendritic shaft. Many

* Corresponding author at: Av. 25 de Mayo s/n y Francia. Campus Miguelete, San Martín (zip code 1650), Instituto de Investigaciones Biotecnológicas (IIB-INTECH), Universidad Nacional de San Martín (UNSAM), Consejo Nacional de Investigaciones Científicas y Técnicas (CONICET), Buenos Aires, Argentina.
E-mail address: cscorticati@iib.unsam.edu.ar (C. Scorticati).

http://dx.doi.org/10.1016/j.mcn.2016.10.005
1044-7431/

neurodegenerative diseases are related to differences in the number and shape of this structure. This affected directly the number of synapses; either an increase or a decrease can be deleterious. For instance, in patients with autism spectrum disorders it has been described an exaggerated spine formation or incomplete pruning leading to increased spine number. In contrast, loss of spine numbers in the adulthood were described in patients with Alzheimer's disease suggesting impaired spine maintenance mechanisms that might underlie cognitive failure (Penzes et al., 2011).

Synaptogenesis involves a complex series of events that promote neuronal differentiation, axon guidance, cell–cell adhesion and local differentiation of pre- and post-synaptic compartments (Shen and Cowan, 2010). Many studies have established that the first step of synaptic contacts between neurons are commanded by filopodia extending from dendrites (Biederer and Stagi, 2008). Consistently, in our laboratory we determined that M6a increases filopodia motility that might actively initiate the synaptic contacts (Brocco et al., 2010). Many membrane proteins like receptor-ligands partners, vesicles containing neurotransmitters and scaffolding proteins are described as synaptic promoter molecules that are present in dendrite as pre and post-synaptic components before the synapse occurs. Afterwards, by cell-cell contact the synaptic component accumulation (puncta) is generated at the synaptic active zone (Chen and Cheng, 2009).

To date, there are only a few experimental evidences suggesting that M6a might be involved in synaptogenesis. In this sense, Cooper et al. determined that M6a localizes in glutamatergic axons from both cerebellar and hippocampal neurons in the adult rat brain (Cooper et al., 2008). In addition, M6a has been isolated from synaptic vesicles of the adult rat brain (Takamori et al., 2006). These observations would suggest that M6a has a pre-synaptic distribution in the adult rat brain. Also, in neurons from double null mice (gpm6a/gpm6b −/−), Mita et al. found that there is a reduction of the axon and the dendrite extensions, which could be rescued by forcing the expression of M6 proteins. The authors reached the conclusion that M6 proteins are redundantly required for proper axonal outgrowth and pathfinding (Mita et al., 2015). However, studies that directly examine the contribution of M6a in synapse formation are still unidentified. The aim of the present work was to examine the role of M6a in synaptogenesis and spine formation. Here, endogenous M6a distributed homogenously in the pre and post- synaptic compartments and partially colocalized with synaptophysin and NMDA-R1. We showed that overexpression of M6a in cultured neurons stimulates the spine formation and increased synaptophysin puncta and NMDA-R1 puncta and the colocalization of both markers.

2. Materials and methods

2.1. Animals

Sprague–Dawley female rats maintained at the Facultad de Ciencias Veterinarias of the University of Buenos Aires (FVET-UBA) were used. All animal procedures were carried out according to the guidelines of the National Institutes of Health (publications No. 80-23) and the Committee for the Care and Use of Laboratory Animals of the Universidad de San Martín (CICUAE-UNSAM No. 03/2015) (Buenos Aires, Argentina).

2.2. Reagents and antibodies

F-Actin filaments were stained with rhodamine-conjugated phalloidin (1/1000, Molecular Probes, Eugene, OR, USA). Primary antibodies were: monoclonal anti-M6a rat IgG (M6a-mAb 1/250) (Medical and Biological Laboratories, Nagoya, Japan), monoclonal anti-β-tubulin III (Tuj-1, 1/1000, Covance, Princeton, USA) and monoclonal mouse anti-microtubule associated protein type 2 (MAP-2) IgG (1/1000, Sigma, St. Louis, MO, USA). Polyclonal antibodies against synaptophysin rabbit IgG (1/500) and monoclonal mouse antibodies against *N*-methyl-D-aspartate receptor type 1 (NMDA-R1, 1/500) purchased from Synaptic Systems GmbH (SySy, Goettingen, Germany). Preabsorbed secondary antibodies were: Alexa fluor 633 goat anti-mouse IgG (1/1000), Alexa fluor 647 goat anti-mouse IgG (1/1000), Alexa fluor 568 goat anti-rabbit IgG (1/1000), and Alexa fluor 488 donkey anti-rat IgG (1/1000) all purchased from Invitrogen Corporation (Invitrogen, Leiden, the Netherlands).

2.3. Plasmids

For green fluorescent protein (GFP)-tagged proteins, a plasmid encoding for GFP (EGFP-*C*1; Clontech Laboratories, Palo Alto, CA, USA) fused in frame with the sequence encoding M6a was used. The coding sequence of M6a was cloned between the *ApaI* and *KpnI* sites of the plasmid. The plasmid encoding membrane GFP (mGFP) was obtained from Adgene. The mutants SNP1 (F93C, rs11545190) and SNP2 (I97S, rs11729990) were generated in a M6a:EGFP-*C*1 vector by standard PCR mutagenesis techniques using BD Advantage 2 Polymerase Mix (BD Biosciences Clontech, Heidelberg, Germany). Two overlapping oligonucleotides containing the target mutation (Macrogen Inc., Korea) were used to amplify the template DNA. *DpnI* endonuclease (New England Biolabs, Ipswich, USA) was used to digest the parental DNA template and select for novel synthesized DNA containing mutations. The identity of all constructs was verified by DNA sequencing (Formoso et al., 2015).

2.4. Hippocampal cultures and plasmid transfection

Dissociated neuronal cultures were prepared from rat hippocampi of embryonic day 19, as previously described (Formoso et al., 2015). Briefly, tissues were treated with 0.25% trypsin in Hanks' solution at 37 °C for 15 min. A single-cell solution was prepared in Neurobasal® medium (NB, Invitrogen) containing 2 mM glutamine (Sigma), 100 units/ml penicillin, and 100 μg/ml streptomycin (NB1X) with 10% (v/v) horse serum (Gibco®, Thermo Fisher Scientific). Cells were seeded on coverslips coated with 0.1 mg/ml poly-L-lysine hydrobromide (Sigma) and 20 mg/ml laminin (Invitrogen) at a low density of 7000 cells per well into a 24 plate. After 2 h, the medium was changed to NB/N2 (NB1X with 1 g/L ovalbumin; N2 and B27 serum-free supplements from Invitrogen). Based on morphological characteristics, we estimated that >90% of the cells in the cultures were neurons.

2.5. Synapses: immunocytochemistry-based assay

To assess synapse formation mediated by M6a, we performed three experiments. Firstly, we evaluated the endogenous distribution of M6a in primary hippocampal neurons along a time curve (1–15 days in vitro –DIV-) to establish whether there is a polarity in the distribution of M6a between pre- and post-synaptic compartments. Secondly, we analyzed the presence, number and type of dendritic spines. Lastly, we evaluated synapse formation by labeling pre- and post-synaptic proteins (Ippolito and Eroglu, 2010). All the experiments were developed at a low density of neurons (7000 neurons/well) in 24-well plates. Each independent experiment is represented by three coverslips to avoid a bias between small density differences among groups. The selected neurons should be at least two cell diameters away from their nearest neighbor. All experiments were carried out under blind conditions to the examiner. Spine morphology and synapse formation were determined from 12 to 14 DIV neurons transfected with mGFP or M6a-GFP or *GPM6A* variants-GFP by the calcium phosphate method (Vogl et al., 2015). Briefly, 3 μg of DNA mixed with 2.5 μl of calcium chloride (2 M, pH: 7.2) and H_2O q. s. 25 μl per well. While this solution was dropped into a tube with 25 μl of HBS 2× solution (HEPES 50 mM, Na2HPO4 1.5 mM, NaCl 280 mM, pH: 7.1), the mixture was bubbled with a Pasteur pipette and incubated for 15–30 min at 25 °C.

Then, 40 μl of the suspension was dropped into each well and incubated for 4–6 h at 37 °C. Cells were washed five times for 5 min with PBS prewarmed at 37 °C and incubated in conditioned medium. As in the case of mGFP-overexpressing neurons, M6a-, SNP1- and SNP2-overexpressing cells showed equal amounts of the protein and correct localization on the neuron surface, as previously reported (Formoso et al., 2015).

2.6. M6a endogenous distribution

Depending on the stage of development, 1–4 DIV, 7 DIV, 10 DIV and 15 DIV neurons were incubated with anti-M6a mAb in fresh medium for 1 h at 4 °C. After a PBS wash, neurons were labeled with anti-rat Alexa 488 (1:1000) for 1 h at 4 °C. Afterwards, neurons were subjected to two different protocols.

In the first protocol, 1–4 DIV, 7 DIV, 10 DIV and 15 DIV neurons were fixed with 4% PFA, 2% sucrose in PBS, permeabilized with 0.1% Triton X-100 and blocked with 3% BSA diluted in PBS for 1–2 h at 25 °C. Afterwards cells were labeled with either monoclonal Tuj-1, for 1–4 DIV cells or monoclonal anti-MAP-2 for 7, 10 and 15 DIV cells at 4 °C. Secondary antibody incubation was carried out with anti-mouse Alexa 633 and actin filaments were stained with phalloidin-rhodamine for 1 h at 25 °C.

In the second protocol, 7, 10 and 15 DIV neurons were fixed with a solution containing 90% methanol and 10% buffer MES (100 mM MES pH 6.9, 1 mM EGTA, 1 mM MgCl2) for 10 min at 4 °C. Cells were washed with PBS-Tween (0.1%) for 5 min. The first blocking solution used was FBS-Triton X-100 (FBS 10%, Triton X-100 0.1% diluted in PBS). The second blocking solution was 3% BSA diluted in PBS for 20–30 min at 25 °C. Both blocking solutions were centrifuged at maximum velocity for 10 min. Neurons were stained with mouse anti-NMDA-R1 for 12–16 h at 4 °C and rabbit anti-synaptophysin. Both primary antibodies were diluted in PBS-BSA 1% solution and centrifuged for 10 min at maximum velocity followed by three washes with PBS. Cells were blocked again with 3% BSA and then with 10% FBS, Triton X-100 0.1% PBS for 1 h at 25 °C followed by the incubation with the secondary antibodies anti-mouse Alexa 633 and anti-rabbit Alexa 568. Secondary antibodies were diluted at 1:1000 in 1% BSA:PBS previously centrifuged for 10 min at maximum velocity. Coverslips were mounted in Fluorsave ® (Calbiochem). Fluorescence images were acquired with a confocal microscope Olympus FV1000 attached to an inverted microscope Olympus IX81 (Melville, NY, USA). FluoView software (version 3.3, Olympus) was used to acquire sequential images with a 60× objective with a NA 1.42. The 2× digital zoom was used and the pixel size of the images was 1600 × 1600, following the Nyquist criterion.

2.7. Synapse quantification by immunostaining

The day after transfection, neurons were fixed with a solution containing 90% methanol and 10% MES buffer (100 mM MES pH 6.9, 1 mM EGTA, 1 mM MgCl2) for 10 min at 4 °C. Cells were washed with PBS-Tween (0.1%) for 5 min. The cells were fixed and stained with mouse anti-NMDA-R1 and rabbit anti-synaptophysin as explained above. Cells were incubated with secondary antibodies anti-mouse Alexa 647 and anti-rabbit Alexa 568, which were diluted at 1:1000 in 1% BSA in PBS and centrifuged for 10 min at maximum velocity. Coverslips were mounted in Fluorsave ®. Fluorescence images were acquired as describe above.

2.8. Image procedures and analysis

Synapse formation was measured by detecting colocalized puncta, in 25 μm of dendrite length, between post- and pre-synaptic markers in approximately 20–30 neurons per condition (approximately 10 per coverslip), using 2–3 fragments per neuron. This means each fragment was treated as an individual value. These colocalized puncta were determined using the plugin Puncta analyzer from Image J (NIH, 1.28 version) (Ippolito and Eroglu, 2010). At least three independent experiments were measured. Images were processed in Adobe Photoshop (version 8.0.1; Adobe Systems, San Jose, CA, USA).

2.9. Study of the morphology and number of dendritic spines

The day after transfection, neurons were fixed with a solution containing 4% PFA, 4% sucrose diluted in PBS at 4 °C for 10 min followed by three washes with pre-chilled PBS for 5 min each. Coverslips were mounted with Fluorsave®. Spine density was quantified separately for segments of selected second- or third-order dendritic branches and imaged with a confocal laser microscope Olympus FV1000 attached to an inverted microscope Olympus IX81 (Melville, NY, USA). Confocal images were acquired in sequential mode with FluoView (version 3.3, Olympus). Stacks series, with 0.10 μm slice thickness, were taken with a zoom of 4× and a 60× lens (1.42 NA) collected from the bottom to the top, covering all dendrites and protrusions. We used an image size of 1024 × 1024 pixels and a scan speed of 4 μs/pixel. The number of spines and the dendritic length were measured using the ImageJ software. The number of spines was normalized per 10 μm of dendritic length and a minimum of three dendrites per cell (10–15 cells per group) were analyzed in at least three independent experiments. For the 3D visualization of the z-stacks, we used the FIJI software based on the ImageJ software (NIH). The spines sampled from the dendritic segments were classified as immature (filopodia, long-thin, stubby) or mature (mushroom, or cup-shaped) (see Fig. 4B) based on their morphological characteristics, including the combination of spine length, width, presence of head and relative width of the head (Hering and Sheng, 2001; Nimchinsky et al., 2002).

2.10. Statistical analysis

Statistical analysis was performed using Student's *t*-test or one-way ANOVA, followed by Bonferroni's post hoc test. $P < 0.05$ was considered statistically significant. Calculations were performed with GraphPad Prism 5.0 (San Diego, CA, USA) and data are expressed as mean + SEM.

3. Results

3.1. Endogenous M6a colocalizes with both pre and post-synaptic markers

To determine whether endogenous M6a is able to influence the formation of synapses, its cellular distribution along neuronal development in cultured hippocampal neurons was analyzed. Fig. 1 shows representative images of neurons at different stages of development (1–15 DIV) labeled with rat anti-M6a-mAb (shown in green), mouse anti-β-tubulin III as a neuronal marker in 1–4 DIV neurons (Tuj-1, shown in blue) or mouse anti-MAP-2 as a dendrite marker in 7–15 DIV (shown in blue), and rhodamine phalloidin as F-actin probe conjugated (shown in red). We found that M6a is distributed in dots throughout the neuronal membrane of the soma (insets f and h) and primary neurites (insets a–e and g). M6a depicted a uniform distribution at all stages of development and shows no distinction between neurites and axons, being especially restricted at the edge of both processes (insets a and g). In addition, M6a is present in filopodia protrusions that partially colocalized with F-actin (1, 2, 3 and 4 DIV), as we have previously reported (Alfonso et al., 2005a). Similarly, at 7, 10 and 15 DIV, M6a is evenly dot-shaped distributed along the entire neuronal surface, showing no preference for pre-synaptic (axons positive for M6a and F-actin but negative for MAP-2) or post-synaptic (dendrites and spines) regions (insets h–i).

We visualized synapses by immunocytochemistry as points of colocalization between clusters of post-synaptic receptors and clusters of synaptic vesicle proteins. In this case, we analyzed whether M6a shows points of colocalization with pre and post synaptic

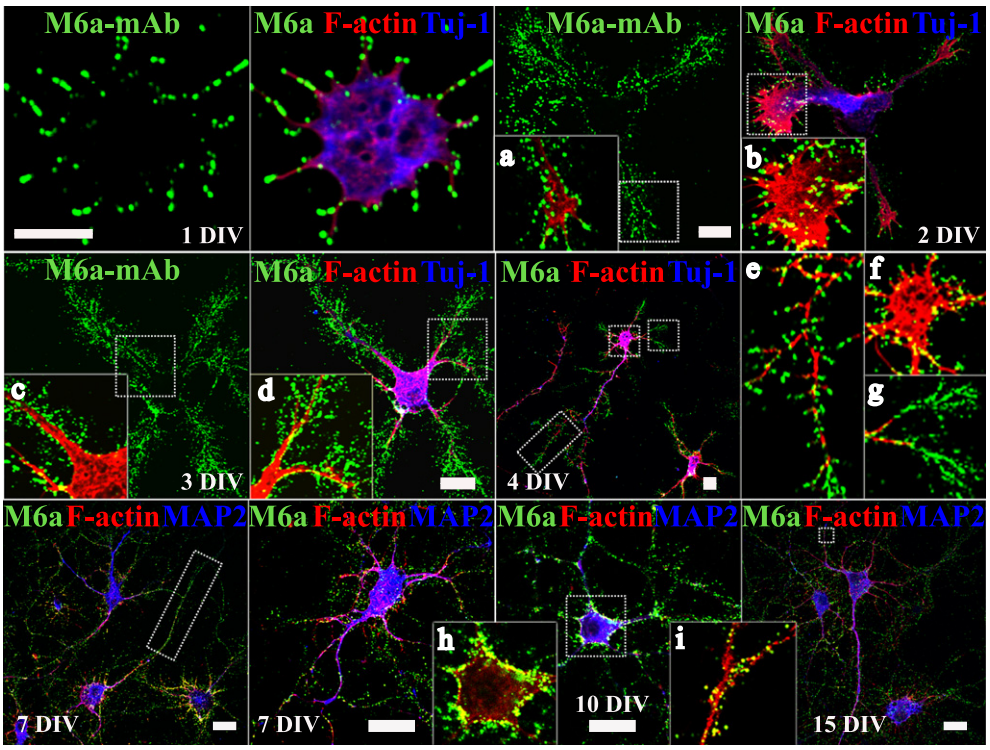

Fig. 1. Endogenous M6a is distributed homogenously all along the neuron surface. Primary hippocampal neurons were plated and cultured for 1–15 DIV. Representative fluorescence images from confocal microscopy show neurons immunostained with anti-M6a-mAb (shown in green) and phalloidin (F-actin, shown in red). At 1–4 DIV, neurons were also labeled with an anti-β-tubulin III antibody (Tuj-1) as a neuronal marker, whereas at 7–15 DIV, neurons were labeled with anti-MAP-2 as a dendrite marker both (shown in blue). The magnifications show a fragment (a–i), indicated by white square, stained only with anti M6a-mAb (green) and F-actin (red). a) Primary neurites and b) neuronal growth of a 2 DIV neuron; c–d) neurites and filopodia of a 3 DIV neuron and e) axon f) soma and g) neurites of a 4 DIV neuron. h) Soma of a 10 DIV neuron and i) dendrite spines of a 15 DIV neuron. Scale bar: 10 μm and the insets size are a–g) 15 × 15 μm and h-i) 10 × 10 μm.

markers (Fig. 2A) by using dissociated hippocampal neurons at 15 DIV labeled with mouse anti-NMDA-R1 antibody as the post-synaptic marker (shown in blue), rabbit anti-synaptophysin antibody as the pre-synaptic marker (shown in red) and rat anti-M6a-mAb (shown in green). Fig. 2A shows a representative image of a 15-DIV neuron and its magnifications (15 μm-long primary or secondary dendrites, a–d), where M6a colocalized with synaptophysin (yellow arrowhead, b–c) and NMDA-R1 (light blue arrowheads, b and d). Moreover, we observed points of triple colocalization (white arrowheads, a–b), which led us to speculate a functional participation of M6a in synaptogenesis. Accordingly, we analyzed the puncta colocalization between M6a, NMDA-R1 and synaptophysin. Fig. 2B–C shows a representative image of 20 μm of dendrite length showing the colocalization between i) synaptophysin clusters and NMDA-R1 clusters (Syn/NMDA-R1, magenta asterisks), ii) synaptophysin clusters and M6a clusters (Syn/M6a, yellow asterisks), and iii) NMDA-R1 clusters and M6a clusters (M6a/NMDA-R1, light blue asterisks). The output obtained from the Puncta Analyzer is represented as black squares. In other words, each black square represents the colocalization puncta between the markers indicated in the image (magnified in the insets). Fig. 2B shows the colocalization puncta of Syn/NMDA-R1, Syn/M6a and M6a/NMDA-R1 that coexist (white asterisks). Moreover, there are points of colocalizating puncta of M6a/NMDA-R1 in the absence of colocalization with synaptophysin puncta. Fig. 2C shows an example of points of colocalization puncta between the three possible pairs that are independent from each other. The orange asterisks indicate points where colocalization puncta of Syn/M6a and M6a/NMDA-R1 coexist. These results led us to speculate the functional participation of M6a in synapse formation.

3.2. Neurons overexpressing M6a show an increase in both synaptic puncta markers and likely synapses

We next examined whether M6a could modulate the number of pre and post synaptic components (synaptophysin and NMDA-R1 respectively) and, likely, synapses. Neurons at 15 DIV overexpressing either mGFP or M6a were subjected to immunocytochemistry, as mentioned above for Fig. 2. We quantified the effect of M6a overexpression on the number of colocalizing puncta of pre and post-synaptic proteins as a synapse by using plugin Puncta Analyzer (Ippolito and Eroglu, 2010). The number of synapses was quantified, with a constant threshold, as the synaptic puncta colocalized with each synaptic marker. In cultures of 14–15 DIV neurons, the distribution of synaptophysin-containing puncta along cell bodies and dendrites was consistent with the distribution of pre-synaptic buttons, as seen by electron microscopy. On the other hand, the distribution of NMDA-R1-containing puncta of glutamatergic neurons was consistent with post-synaptic compartments (Fletcher et al., 1991; Weiss et al., 1998). Fig. 3A shows representative images of 25 μm dendritic segments of each group. For a better visualization of the spots of colocalization, dendritic segments overexpressing mGFP or M6a are shown in gray; synaptophysin was stained in red and NMDA-R1 was stained in deep red (shown in green). Neurons overexpressing mGFP show few points where the red mark is aligned with the green mark (colocalization observed in yellow). In contrast, neurons overexpressing M6a show a significant larger number of yellow points all along the dendrite shaft and spines. The plugin provides the quantification corresponding to the puncta of each marker separately and the puncta colocalized with each of them. Fig. 3B–D shows the quantification of the number of synaptophysin, NMDA-R1 and colocalization puncta as possible synapses respectively. In all

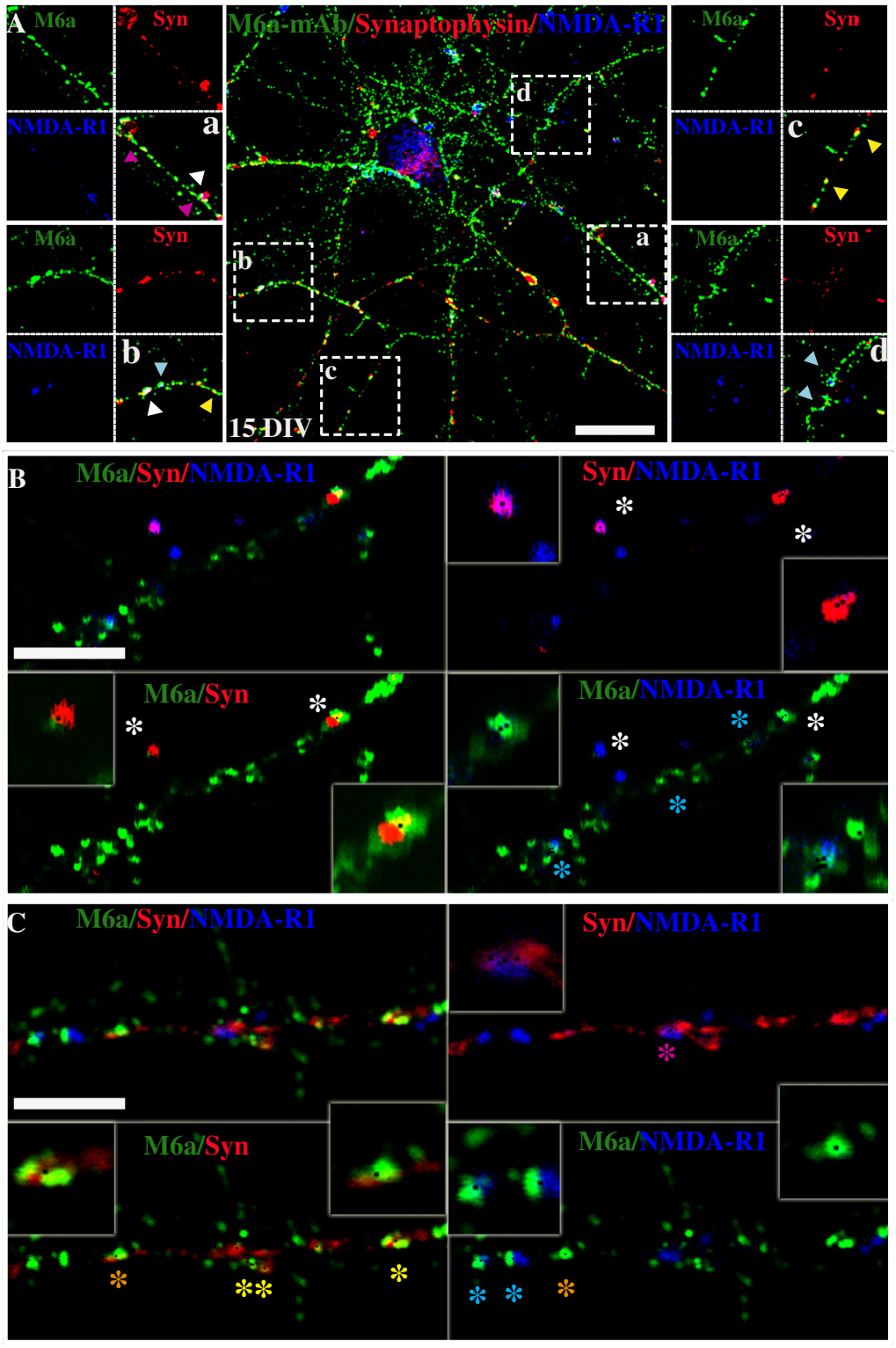

Fig. 2. Endogenous M6a colocalizes with both pre-synaptic and post-synaptic markers. (A) Representative images of a 15 DIV hippocampal neuron labeled with anti-M6a-mAb (green), the pre-synaptic marker synaptophysin (Syn, in red) and the post-synaptic marker NMDA-R1 (in blue). Colocalization of proteins of M6a; Syn and NMDA-R1 in 15 μm of dendrite length is shown in the magnifications. Colour arrowheads indicate colocalization of the labeled proteins: white arrowheads represent triple colocalization, light blue arrowheads represent M6a/NMDA-R1 colocalization, yellow arrowheads represent M6a/Syn colocalization and magenta arrowheads represent Syn/NMDA-R1 colocalization. Scale bar: 15 μm. (B and C) Magnification from 20 μm of dendrite labeled as described in A. Scale bar: 5 μm. The output obtained from the Puncta Analyzer is represented as black squares (magnified in the insets). (B) Colocalization puncta of Syn/NMDA-R1 (magenta asterisks), Syn/M6a (yellow asterisks) and M6a/NMDA-R1 (blue light asterisks) simultaneously plotted (white asterisks). (C) Points of colocalization puncta between the three possible pairs that are independent from each other. The orange asterisks indicate points of colocalization puncta of Syn/M6a and M6a/NMDA-R1.

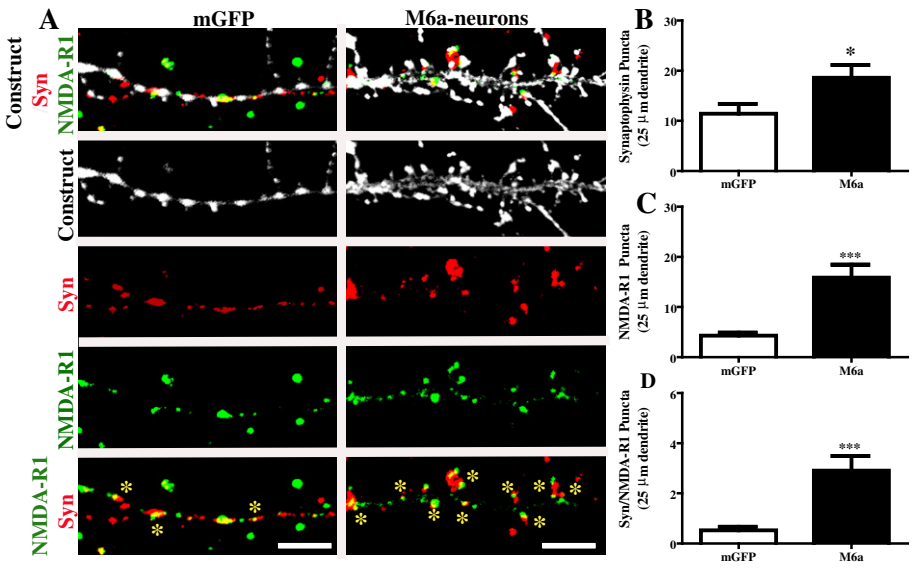

Fig. 3. Neurons overexpressing M6a show an increase of both synaptic puncta markers and likely synapses. (A) Representative images of segments of 25 μm of a dendrite from 15 DIV neurons show the distribution of the construct shown in gray. Neurons were labeled for synaptophysin (Syn in red) and NMDA-R1 (green). Merged images show yellow dots that represent overlapping of the clusters of pre- and post-synaptic markers. Asterisks represent the overlapping (yellow). Scale bar: 5 μm. (B-C) Puncta Analyzer quantification of clusters was done along 25 μm of dendrite. (D) Clusters of colocalization of synaptophysin and NMDA-R1 as average number of likely synapses. White bars represent mGFP and black bars represent M6a:GFP. Significant differences were determined using Student's *t*-test. ***, $p < 0.005$, and * $p < 0.05$ mGFP vs M6a. The data show a representative experiment of three independent experiments, where each bar represents the mean of the total of fragments of 25 μm of dendrite length, and are expressed as mean + SEM.

cases, M6a-overexpressing neurons presented a significantly higher average number of synaptophysin puncta, NMDA-R1 puncta and colocalized puncta than mGFP-overexpressing neurons. The results obtained here suggest that M6a modulates excitatory synapses by increasing both synaptic components that possibly increase the synapse number.

3.3. Neurons overexpressing M6a show an increase in spine density

Dendritic spines appear as small protrusions (<2 μm in length from dendrite shaft to the tip) that play a major role in neuronal plasticity and integration throughout their structural reorganization. We have previously shown that M6a promotes filopodia formation in different cell

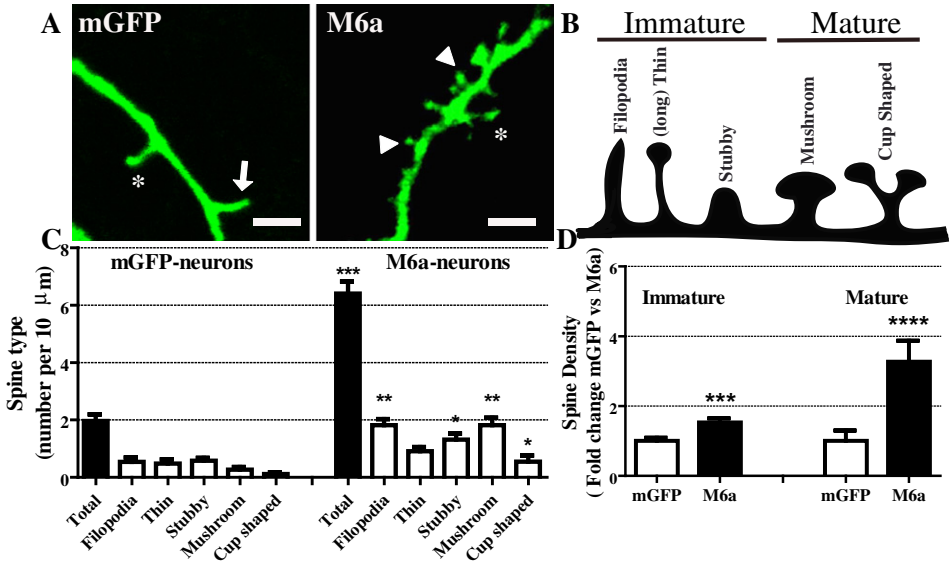

Fig. 4. M6a-overexpression increases dendritic spine density. (A) Representative images of second/tertiary dendrite segments (10 μm in length) from neurons at 15 DIV expressing mGFP or M6a:GFP. According to spine morphology, asterisks indicate long-thin, arrows indicate filopodia, and arrowheads indicate mushrooms. Scale bar: 2 μm. (B) Dendritic spine can be classified as stubby, filopodia, long-thin, mushroom and cup-shaped. According to their functionality, they can be also classified as immature (filopodia, long-thin and stubby) or mature (mushroom and cup-shaped). (C) Spines were quantified as the number of spines per 10 μm of dendrite. Black columns represent total spine number and white columns represent the number of each spine type. Student's *t*-test. ***, $p < 0.005$ mGFP vs M6a, **, $p < 0.01$ mGFP filopodia and mushroom vs. M6a filopodia and mushroom, *, $p < 0.05$ mGFP cup-shaped vs M6a cup-shaped. (D) Spine density is shown as fold change mGFP vs. M6a. Significant differences were determined by Student's *t*-test, ****, $p < 0.001$ mGFP mature vs. M6a mature, ***, $p < 0.01$ mGFP immature vs. M6a immature. The data are expressed as mean + SEM and are representative of three independent experiments.

lines (Alfonso et al., 2005a; Fuchsova et al., 2009). Here, we analyzed whether M6a might be involved in dendritic spine formation. For that purpose, 14–15 DIV neurons were transfected with mGFP or M6a fused to GFP. Fig. 4A shows representative images of 10 μm of dendritic length of mGFP/M6a-overexpressing neurons. Spine density and morphology were evaluated from three-dimensional visualizations of 10-μm segments of second- or third-order dendritic branches from a minimal of three segments per neuron. Spine morphology is highly variable and, based on their structure, spines can be classified as: filopodia, long-thin, stubby and mushroom-shaped, the latter of which includes mushroom, cup-shaped or branched. On the other hand, some authors classify them in immature and mature taking into consideration that a mature spine has a mushroom-like shape (Kasai et al., 2010) (Fig. 4B). The total average number of spines in M6a-overexpressing neurons was significantly higher than the control group. Taking the spine shape and length into account, we established that M6a-overexpressing neurons have a significant change in the number of both immature spines (filopodia and stubby) and mature spines (mushroom and cup-shaped) (Fig. 4C). For this reason, we analyzed differences within mature and immature groups. The results obtained show that mature spines predominate in M6a-overexpressing neurons, which show a 2.5-fold increase over mGFP-overexpressing neurons, compared with immature spines, which show a 1.5-fold increase over mGFP-overexpressing neurons (Fig. 4D). Taken together, these results show that M6a promotes spine formation in cultured hippocampal neurons, with a majority of mature spines.

3.4. Neurons overexpressing GPM6A variants impair the number of synaptic puncta markers and likely synapses

In a previous work, we analyzed the effect of different genetic variants in the coding region of the human *GPM6A* gene. We focused on protein stability, dimerization and function. Particularly, two nsSNPs located in TMD2 (SNP1 (rs11545190, F93C) and SNP2 (rs11729990, I97S)) affect M6a stability, self-interactions and filopodia induction in neurons at 5 DIV (Formoso et al., 2015) (Fig. 5B). In this work, we explored whether these nsSNPs might modify M6a synapse promotion by immunocytochemistry synapse assay in cultured neurons. Therefore, at 15 DIV, neurons overexpressing either mGFP, M6a, SNP1 or SNP2 were subjected to immunofluorescence, as mentioned above for Fig. 3A. Fig. 5A shows representative images of 25 μm of dendritic segments of each construct (in gray) showing stained clusters of synaptophysin in

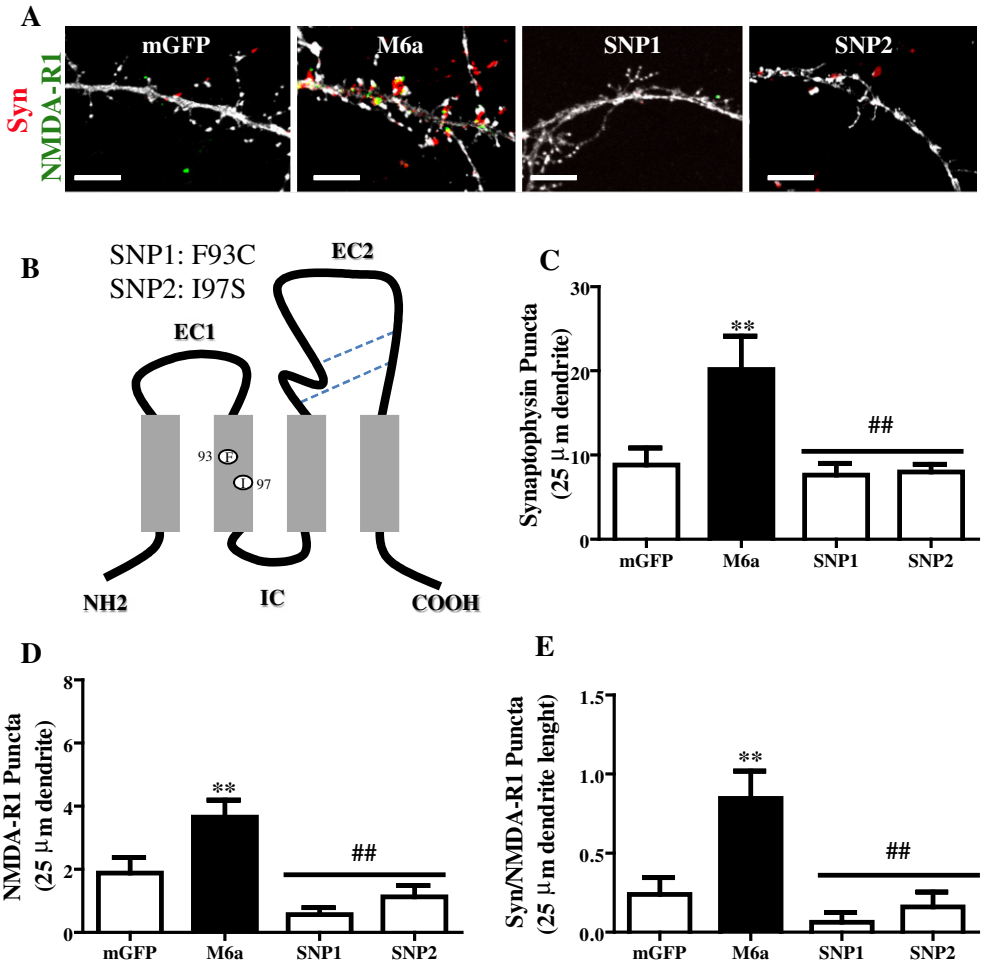

Fig. 5. Neurons expressing *GPM6A* variants impair the number of both pre- and post-synaptic puncta markers and likely synapses. (A) Representative images of dendrite fragments of 25 μm of 15 DIV neurons show the constructs mGFP, M6a, SNP1 (rs11545190, F93C) or SNP2 (rs11729990, I97S) in gray, synaptophysin in red and NMDA-R1 in green. The yellow puncta in the images show the overlapping of the clusters of pre- and post-synaptic markers. Scale bar: 5 μm. (B) Topological prediction of M6a structure. M6a possesses four transmembrane domains (TMDs), one minor (EC1) and one major (EC2) extracellular loop, one intracellular (IC) loop and the N- and C-terminal regions facing the cytoplasm. Highlighted are the different genetic variants assayed in this work. The white circles indicate the relative positions of the two nsSNPs located in *GPM6A* TMD2 identified in the dbSNP database. (C-D) Cluster were quantified by means of the Puncta Analyzer along 25 μm of dendrite. (E) Clusters of colocalization of synaptophysin and NMDA-R1 as average number of synapses. Black bars represent M6a-overexpressing neurons. Significant differences were determined by Student's *t*-test. **, $p < 0.01$ mGFP vs. M6a; ##, $P < 0.01$ M6a vs. SNP1 and SNP2. The data show a representative experiment of three independent experiments, where each bar represents the mean of the total of fragments of 25 μm of dendrite length, and are expressed as mean + SEM.

red and NMDA-R1 in green. Neurons overexpressing wild type (wt) M6a showed several points of colocalization (shown in yellow) compared to mGFP-overexpressing neurons or both mutants, which showed few points of colocalization. The quantification of the average number of (synaptic markers) puncta and the colocalization of both are shown in Fig. 5C–E. As in the case of Fig. 3B–D, the number of synaptic markers (synaptophysin and NMDA-R1) puncta in M6a-overexpressing neurons is significantly higher than in mGFP-overexpressing neurons. However, neurons overexpressing the SNP1 and SNP2 variants have the same number of clusters of synaptic markers as control neurons. Moreover, the quantitative analysis of the average number of colocalized puncta of both synaptic markers showed that none of the SNPs were able to induce synapses compared with M6a-neurons. In fact, the number of synapses detected in neurons overexpressing either SNP was significantly lower than that in M6a-overexpressing cells (Fig. 5E). These results confirm the deleterious functional effect of the missense mutations in the human *GPM6A* gene.

3.5. nsSNPs in GPM6A affect M6a spine induction

Based on the latter observations, we then examined whether the nsSNPs in the coding region of *GPM6A* could modify spine arborization in mature cultured neurons. As explained for Fig. 4, at 14–15 DIV, neurons were transfected with mGFP, M6a, SNP1 or SNP2 fused to GFP. The day after, cells were fixed and mounted to evaluate changes in spine density, morphology and function. Fig. 6A shows a panel of representative images of 3D visualization of 10 μm of secondary or tertiary dendritic segments transfected with the different constructions (in gray). In the resulting quantification (Fig. 6B–C), as in the case of Fig. 4C–D, wt M6a-overexpressing neurons significantly increased the total number of spines, predominantly mature, compared with mGFP-overexpressing neurons. By contrast, neurons overexpressing the gene variants SNP1 and SNP2 totally blocked the effect of M6a on spine induction. Moreover, in the morphology-functional analysis, both nsSNPs showed levels of immature and mature spines equal to those of mGFP-overexpressing neurons (Fig. 6C).

4. Discussion

In this work, we provide new evidence of M6a synaptic localization in cultured hippocampal neurons. We show that M6a overexpression in neurons modulates dendritic spine arborization/morphology and contributes to cell-cell attachment and consequently might promote

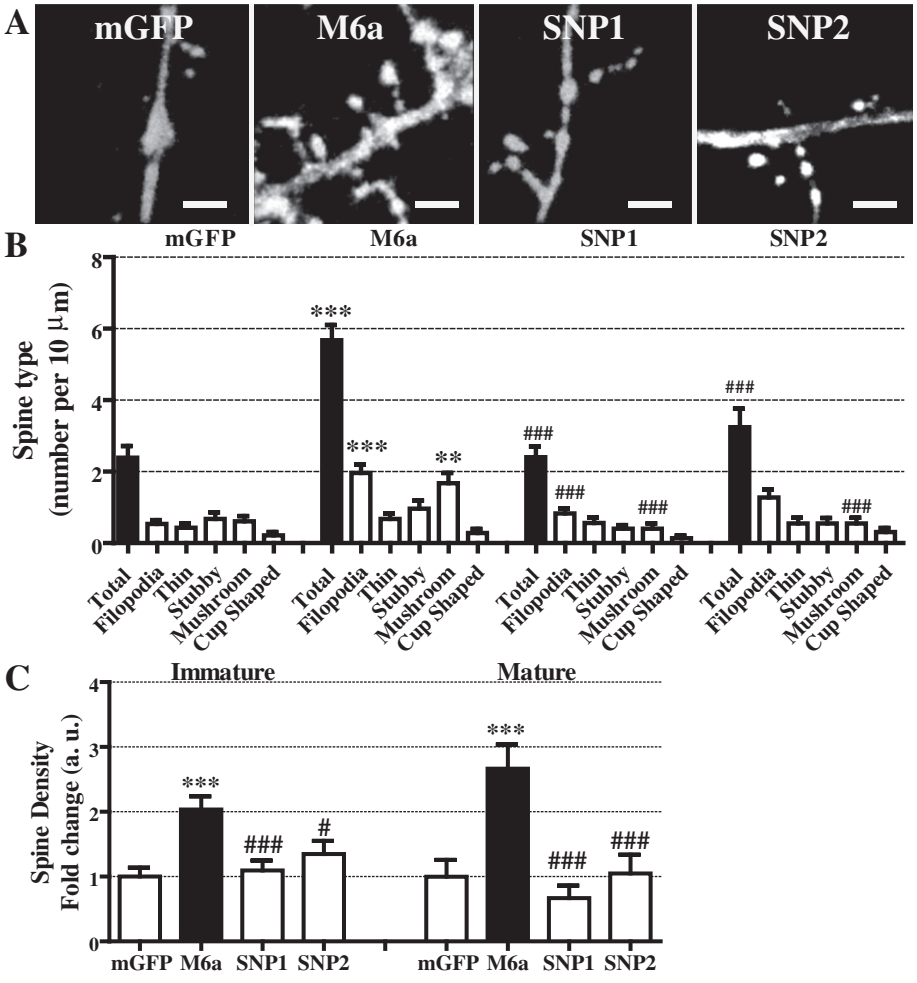

Fig. 6. nsSNPs present in the coding region of *GPM6A* impair spine induction. (A) Representative images of dendrite segments of 10 μm of 15 DIV neurons expressing mGFP, M6a, SNP1or SNP2 neurons are shown in gray. Scale bar: 2 μm. (B) Spine quantification is shown as the number of spines per 10 μm of dendrite. Black columns represent the total number of spines per condition and the white columns represent the number of spines classified by shape per condition. At least three dendrite segments per neuron in almost 20 neurons were quantified. Significant differences were determined by one-way ANOVA, followed by Bonferroni's post-hoc test. ***$P < 0.005$ mGFP vs. M6a and mGFP filopodia vs. M6a filopodia; **, $p < 0.01$ mGFP mushroom vs. M6a mushroom; ###, $P < 0.005$ M6a vs. SNP1- and SNP2-expressing cells, M6a filopodia vs. SNP1 filopodia and M6a mushroom vs. SNP1/SNP2 mushroom. (C) Spine density is shown as fold change mGFP vs. M6a, SNP1 or SNP2. ***$P < 0.005$ mGFP immature vs. M6a immature and M6a immature vs. M6a mature. ###, $P < 0.005$ M6a immature vs. SNP1 immature; ###, $P < 0.005$ M6a mature vs. SNP1 and SNP2 mature. #, $P < 0.05$ M6a immature vs. SNP2. The data are expressed as mean + SEM and are representative of three independent experiments.

synapse formation. We also described the potential deleterious risk of two genetic variants (nsSNPs) reported in the human *GPM6A* gene.

Since the way in which M6a is distributed within different synaptic compartments is unknown, we first conducted a study to visualize M6a endogenous distribution in hippocampal neurons at different stages of development. Cooper et al. determined that M6a had an exclusive pre-synaptic localization in axons of glutamatergic neurons in the adult rat brain (Cooper et al., 2008). Moreover, by means of electron microscopy, Roussel et al. detected M6a only in the cytoplasmic side of the pre-synaptic membrane and in the membrane of synaptic vesicles in granular cells from the cerebellum of young rats (Roussel et al., 1998). Consistently, by using mass spectrometry Takamori et al. determined that M6a is present in synaptic vesicles purified from adult rat brain (Takamori et al., 2006). Here, we showed that endogenous M6a in neurons across 4–15 DIV does not have a predominantly axonal distribution as reported in the rat brain, but rather a uniform staining along the neuronal surface. Moreover, M6a showed points of colocalization puncta with both pre- and post-synaptic markers. These results suggest different possibilities: i) M6a could be part of the pre-synaptic boutons that are closely related to synapses in which NMDA-R1 is involved; ii) M6a could be part of the post-synaptic compartments in association with synapses in which synaptophysin is involved; iii) M6a can be part of both pre- and post-synaptic compartments and its distribution differs from that observed in the brain tissue. To further address these possibilities, techniques such STED or STORM should be used (Dani et al., 2010). The same behavior has been reported for brain-derived neurotrophic factor (BDNF). Results of studies in neurons overexpressing BDNF suggest that it is closely related to pre- and post-synaptic compartments. However, in the case of brain sections, endogenous BDNF has been found only in pre-synaptic sites (Andreska et al., 2014).

Although synapse formation is a complex process that has been widely studied, the mechanisms of action have not been fully described. In this sense, neither spine formation nor the types of dendritic spines that may participate in a synapse have been fully determined. Thus, three possible models have been proposed to explain how a synapse is established. Sotelo's model describes that a synapse could arise when a stubby spine is contacted by the axon terminal and induces its development towards the mushroom type (Sotelo et al., 1975). In Miller/Peters's model, the pre-synaptic terminal could directly contact with the dendrite shaft, inducing spine outgrowth (Miller and Peters, 1981). Finally, in the Filopodial model, dendritic filopodia may actively initiate synaptogenic contacts by contacting a pre-synaptic terminal that would induce its stabilization and thereafter mature to the mushroom type (Yuste and Bonhoeffer, 2004; Ziv and Fisher-Lavie, 2014).

The ideal assay to measure a functional synapse is one that tests both the pre-synaptic and post-synaptic function. Here, we quantified synapses by the immunoreactivity of molecular components (clusters of post-synaptic receptors opposed to clusters of synaptic vesicle proteins) (Craig et al., 2006). We measured the synaptogenic effect of M6a using the Puncta analyzer in neurons (Ippolito and Eroglu, 2010). The number of both synaptophysin and NMDA-R1 clusters was higher in M6a-overexpressing neurons than in mGFP-overexpressing ones. Furthermore, the average number of possible synapses placed in the dendrite shaft and spines was significantly greater than in control cells. In agreement, we have previously reported significantly lower density of pre-synaptic clusters of synaptophysin in neurons treated with RNA interference to deplete endogenous M6a (Alfonso et al., 2005a). Besides, dendrites that are in contact with M6a-transfected axons show high quantity of synaptophysin clusters (Fuchsova et al., 2009). Here, we first established an induction of synaptophysin and NMDA-R1 clusters in M6a-overexpressing neurons and points of double colocalization of both synaptic markers positioning M6a as possible promoter of synapses. However, these findings should be corroborated with electrophysiology or electron microscopy.

M6a has been linked to various psychiatric disorders such as schizophrenia, bipolar depression and claustrophobia (Boks et al., 2008; El-Kordi et al., 2013; Fuchsova et al., 2015). It has been described that in many neurodegenerative diseases, including depression, Alzheimer, and Parkinson, there is either a decrease or an increase in spine density and/or in the proportion of mature and immature spines (Lopes et al., 2015; Mavroudis et al., 2013; Sierakowiak et al., 2014; Yang et al., 2012). The results obtained here show that M6a promotes dendritic spines in primary cultured neurons of 15 DIV. In addition, we evaluated the morphology of spines by classifying them as immature (filopodia, long thin and stubby) or mature (mushroom and cup-shaped) (Bae et al., 2012; Kasai et al., 2003; Nimchinsky et al., 2002; Spiga et al., 2014). However, to date, there is no consensus on which dendritic spines are able to participate in synapses. In this sense, our results showed that M6a is able to induce both immature and mature spines, being the latter the main ones. Considering the three models described above, we can only speculate that the increased spine density in M6a-overexpressing neurons eventually might increase synapses formation.

We have previously described that two nsSNPs located in TMD2 of the human *GPM6A* gene impair M6a filopodia induction, stability and dimer formation (Formoso et al., 2015). We have to take into consideration that none of these nsSNPs have a reported frequency, although SNP2 is validated by both HapMap database and Cluster. However, the consequences of missense mutations in the protein's function are important to determine a possible risk for the patients that bear these genetic variants. Indeed, here, the presence of both nsSNPs blocked M6a dendritic spines and synapse formation. It has been reported that animal models of chronic stress/depression display a reduction of dendritic branching and loss of synapses in different areas of the hippocampus (Magarinos et al., 1997; Popoli et al., 2012; Qiao et al., 2016). The reduction of M6a-mRNA expression levels in the hippocampus of chronically stressed mice, tree shrews and depressed humans has been previously reported (Alfonso et al., 2005a; Alfonso et al., 2005b; Cooper et al., 2009; Fernandez et al., 2010; Fuchsova et al., 2015). Thus, we can only ensure that there is a correlation between the significant decrease in spinogenesis and the decrease in the number of synapses, having no distinguishable feature for any of the genetic variants. These synaptic deficits may play an important role as predictor markers in patients with mental disorders who have these variants.

Acknowledgments

We thank Silvia C. Billi Ph D. for excellent technical assistance. KF is a postdoc and M.D.G is PhD student and CS and A.C.F. are researchers from the National Council for Research (CONICET). Contract grant sponsors: CAEN supplies, UNSAM and CONICET grants (to C·S) and Agencia Nacional de Promoción Científica y Tecnológica (to A.C.F.). The authors declare no competing interests. All experiments were conducted in compliance with the ARRIVE guidelines.

References

Alfonso, J., Fernandez, M.E., Cooper, B., Flugge, G., Frasch, A.C., 2005a. The stress-regulated protein M6a is a key modulator for neurite outgrowth and filopodium/spine formation. Proc. Natl. Acad. Sci. U. S. A. 102, 17196–17201.

Alfonso, J., Frasch, A.C., Flugge, G., 2005b. Chronic stress, depression and antidepressants: effects on gene transcription in the hippocampus. Rev. Neurosci. 16, 43–56.

Andreska, T., Aufmkolk, S., Sauer, M., Blum, R., 2014. High abundance of BDNF within glutamatergic presynapses of cultured hippocampal neurons. Front. Cell. Neurosci. 8, 107.

Bae, J., Sung, B.H., Cho, I.H., Kim, S.M., Song, W.K., 2012. NESH regulates dendritic spine morphology and synapse formation. PLoS One 7, e34677.

Biederer, T., Stagi, M., 2008. Signaling by synaptogenic molecules. Curr. Opin. Neurobiol. 18, 261–269.

Boks, M.P., Hoogendoorn, M., Jungerius, B.J., Bakker, S.C., Sommer, I.E., Sinke, R.J., Ophoff, R.A., Kahn, R.S., 2008. Do mood symptoms subdivide the schizophrenia phenotype? Association of the GMP6A gene with a depression subgroup. Am. J. Med. Genet. B Neuropsychiatr. Genet. 147B, 707–711.

Brocco, M.A., Fernandez, M.E., Frasch, A.C., 2010. Filopodial protrusions induced by glycoprotein M6a exhibit high motility and aids synapse formation. Eur. J. Neurosci. 31, 195–202.

Caceres, A., Ye, B., Dotti, C.G., 2012. Neuronal polarity: demarcation, growth and commitment. Curr. Opin. Cell Biol. 24, 547–553.

Chen, S.Y., Cheng, H.J., 2009. Functions of axon guidance molecules in synapse formation. Curr. Opin. Neurobiol. 19, 471–478.
Cooper, B., Werner, H.B., Flugge, G., 2008. Glycoprotein M6a is present in glutamatergic axons in adult rat forebrain and cerebellum. Brain Res. 1197, 1–12.
Cooper, B., Fuchs, E., Flugge, G., 2009. Expression of the axonal membrane glycoprotein M6a is regulated by chronic stress. PLoS One 4, e3659.
Craig, A.M., Graf, E.R., Linhoff, M.W., 2006. How to build a central synapse: clues from cell culture. Trends Neurosci. 29, 8–20.
Dani, A., Huang, B., Bergan, J., Dulac, C., Zhuang, X., 2010. Superresolution imaging of chemical synapses in the brain. Neuron 68, 843–856.
El-Kordi, A., Kastner, A., Grube, S., Klugmann, M., Begemann, M., Sperling, S., Hammerschmidt, K., Hammer, C., Stepniak, B., Patzig, J., de Monasterio-Schrader, P., Strenzke, N., Flugge, G., Werner, H.B., Pawlak, R., Nave, K.A., Ehrenreich, H., 2013. A single gene defect causing claustrophobia. Transl. Psychiatry 3, e254.
Fernandez, M.E., Alfonso, J., Brocco, M.A., Frasch, A.C., 2010. Conserved cellular function and stress-mediated regulation among members of the proteolipid protein family. J. Neurosci. Res. 88, 1298–1308.
Fletcher, T.L., Cameron, P., De Camilli, P., Banker, G., 1991. The distribution of synapsin I and synaptophysin in hippocampal neurons developing in culture. J. Neurosci. 11, 1617–1626.
Formoso, K., Garcia, M.D., Frasch, A.C., Scorticati, C., 2015. Filopodia formation driven by membrane glycoprotein M6a depends on the interaction of its transmembrane domains. J. Neurochem.
Fuchsova, B., Fernandez, M.E., Alfonso, J., Frasch, A.C., 2009. Cysteine residues in the large extracellular loop (EC2) are essential for the function of the stress-regulated glycoprotein M6a. J. Biol. Chem. 284, 32075–32088.
Fuchsova, B., Alvarez Julia, A., Rizavi, H.S., Frasch, A.C., Pandey, G.N., 2015. Altered expression of neuroplasticity-related genes in the brain of depressed suicides. Neuroscience 299, 1–17.
Gartner, A., Fornasiero, E.F., Valtorta, F., Dotti, C.G., 2014. Distinct temporal hierarchies in membrane and cytoskeleton dynamics precede the morphological polarization of developing neurons. J. Cell Sci. 127, 4409–4419.
Greenwood, T.A., Akiskal, H.S., Akiskal, K.K., Kelsoe, J.R., 2012. Genome-wide association study of temperament in bipolar disorder reveals significant associations with three novel loci. Biol. Psychiatry 72, 303–310.
Gregor, A., Kramer, J.M., van der Voet, M., Schanze, I., Uebe, S., Donders, R., Reis, A., Schenck, A., Zweier, C., 2014. Altered GPM6A/M6 dosage impairs cognition and causes phenotypes responsive to cholesterol in human and drosophila. Hum. Mutat. 35, 1495–1505.
Hering, H., Sheng, M., 2001. Dendritic spines: structure, dynamics and regulation. Nat. Rev. Neurosci. 2, 880–888.
Ippolito, D.M., Eroglu, C., 2010. Quantifying synapses: an immunocytochemistry-based assay to quantify synapse number. Journal of Visualized Experiments: JoVE.
Kasai, H., Matsuzaki, M., Noguchi, J., Yasumatsu, N., Nakahara, H., 2003. Structure-stability-function relationships of dendritic spines. Trends Neurosci. 26, 360–368.
Kasai, H., Fukuda, M., Watanabe, S., Hayashi-Takagi, A., Noguchi, J., 2010. Structural dynamics of dendritic spines in memory and cognition. Trends Neurosci. 33, 121–129.
Lagenaur, C., Kunemund, V., Fischer, G., Fushiki, S., Schachner, M., 1992. Monoclonal M6 antibody interferes with neurite extension of cultured neurons. J. Neurobiol. 23, 71–88.
Lopes, J.P., Morato, X., Souza, C., Pinhal, C., Machado, N.J., Canas, P.M., Silva, H.B., Stagljar, I., Gandia, J., Fernandez-Duenas, V., Lujan, R., Cunha, R.A., Ciruela, F., 2015. The role of Parkinson's disease-associated receptor GPR37 in the hippocampus: functional interplay with the adenosinergic system. J. Neurochem. 134, 135–146.
Magarinos, A.M., Verdugo, J.M., McEwen, B.S., 1997. Chronic stress alters synaptic terminal structure in hippocampus. Proc. Natl. Acad. Sci. U. S. A. 94, 14002–14008.
Mavroudis, I.A., Manani, M.G., Petrides, F., Petsoglou, K., Njau, S.D., Costa, V.G., Baloyannis, S.J., 2013. Dendritic and spinal pathology of the Purkinje cells from the human cerebellar vermis in Alzheimer's disease. Psychiatr. Danub. 25, 221–226.
Michibata, H., Okuno, T., Konishi, N., Kyono, K., Wakimoto, K., Aoki, K., Kondo, Y., Takata, K., Kitamura, Y., Taniguchi, T., 2009. Human GPM6A is associated with differentiation and neuronal migration of neurons derived from human embryonic stem cells. Stem Cells Dev. 18, 629–639.
Miller, M., Peters, A., 1981. Maturation of rat visual cortex. II. A combined golgi-electron microscope study of pyramidal neurons. J. Comp. Neurol. 203, 555–573.
Mita, S., de Monasterio-Schrader, P., Funfschilling, U., Kawasaki, T., Mizuno, H., Iwasato, T., Nave, K.A., Werner, H.B., Hirata, T., 2015. Transcallosal projections require glycoprotein M6-dependent neurite growth and guidance. Cereb. Cortex 25, 4111–4125.
Nimchinsky, E.A., Sabatini, B.L., Svoboda, K., 2002. Structure and function of dendritic spines. Annu. Rev. Physiol. 64, 313–353.
Penzes, P., Cahill, M.E., Jones, K.A., VanLeeuwen, J.E., Woolfrey, K.M., 2011. Dendritic spine pathology in neuropsychiatric disorders. Nat. Neurosci. 14, 285–293.
Popoli, M., Yan, Z., McEwen, B.S., Sanacora, G., 2012. The stressed synapse: the impact of stress and glucocorticoids on glutamate transmission. Nat. Rev. Neurosci. 13, 22–37.
Qiao, H., Li, M.X., Xu, C., Chen, H.B., An, S.C., Ma, X.M., 2016. Dendritic spines in depression: what we learned from animal models. Neural Plasticity 2016, 8056370.
Roussel, G., Trifilieff, E., Lagenaur, C., Nussbaum, J.L., 1998. Immunoelectron microscopic localization of the M6a antigen in rat brain. J. Neurocytol. 27, 695–703.
Sato, Y., Mita, S., Fukushima, N., Fujisawa, H., Saga, Y., Hirata, T., 2011a. Induction of axon growth arrest without growth cone collapse through the N-terminal region of four-transmembrane glycoprotein M6a. Dev. Neurobiol. 71, 733–746.
Sato, Y., Watanabe, N., Fukushima, N., Mita, S., Hirata, T., 2011b. Actin-independent behavior and membrane deformation exhibited by the four-transmembrane protein M6a. PLoS One 6, e26702.
Scorticati, C., Formoso, K., Frasch, A.C., 2011. Neuronal glycoprotein M6a induces filopodia formation via association with cholesterol-rich lipid rafts. J. Neurochem. 119, 521–531.
Shen, K., Cowan, C.W., 2010. Guidance molecules in synapse formation and plasticity. Cold Spring Harb. Perspect. Biol. 2, a001842.
Sierakowiak, A., Mattsson, A., Gomez-Galan, M., Feminia, T., Graae, L., Aski, S.N., Damberg, P., Lindskog, M., Brene, S., Aberg, E., 2014. Hippocampal morphology in a rat model of depression: the effects of physical activity. The Open Neuroimaging Journal 9, 1–6.
Sotelo, C., Hillman, D.E., Zamora, A.J., Llinas, R., 1975. Climbing fiber deafferentation: its action on Purkinje cell dendritic spines. Brain Res. 98, 574–581.
Spiga, S., Talani, G., Mulas, G., Licheri, V., Fois, G.R., Muggironi, G., Masala, N., Cannizzaro, C., Biggio, G., Sanna, E., Diana, M., 2014. Hampered long-term depression and thin spine loss in the nucleus accumbens of ethanol-dependent rats. Proc. Natl. Acad. Sci. U. S. A. 111, E3745–E3754.
Takamori, S., Holt, M., Stenius, K., Lemke, E.A., Gronborg, M., Riedel, D., Urlaub, H., Schenck, S., Brugger, B., Ringler, P., Muller, S.A., Rammner, B., Grater, F., Hub, J.S., De Groot, B.L., Mieskes, G., Moriyama, Y., Klingauf, J., Grubmuller, H., Heuser, J., Wieland, F., Jahn, R., 2006. Molecular anatomy of a trafficking organelle. Cell 127, 831–846.
Vogl, A.M., Brockmann, M.M., Giusti, S.A., Maccarrone, G., Vercelli, C.A., Bauder, C.A., Richter, J.S., Roselli, F., Hafner, A.S., Dedic, N., Wotjak, C.T., Vogt-Weisenhorn, D.M., Choquet, D., Turck, C.W., Stein, V., Deussing, J.M., Refojo, D., 2015. Nat. Neurosci. 18 (2):239–251. http://dx.doi.org/10.1038/nn.3912.
Weiss, S.W., Albers, D.S., Iadarola, M.J., Dawson, T.M., Dawson, V.L., Standaert, D.G., 1998. NMDAR1 glutamate receptor subunit isoforms in neostriatal, neocortical, and hippocampal nitric oxide synthase neurons. J. Neurosci. 18, 1725–1734.
Yang, G.Z., Yang, M., Lim, Y., Lu, J.J., Wang, T.H., Qi, J.G., Zhong, J.H., Zhou, X.F., 2012. Huntingtin associated protein 1 regulates trafficking of the amyloid precursor protein and modulates amyloid beta levels in neurons. J. Neurochem. 122, 1010–1022.
Yuste, R., Bonhoeffer, T., 2004. Genesis of dendritic spines: insights from ultrastructural and imaging studies. Nat. Rev. Neurosci. 5, 24–34.
Ziv, N.E., Fisher-Lavie, A., 2014. Presynaptic and postsynaptic scaffolds: dynamics fast and slow. The Neuroscientist: A Review Journal Bringing Neurobiology, Neurology and Psychiatry 20, 439–452.